
ECCCoS from the Black Box: Faithful Explanations through Energy-Constrained Conformal Counterfactuals

Anonymous Author(s)

Affiliation

Address

email

Abstract

Counterfactual Explanations offer an intuitive and straightforward way to explain black-box models but they are not unique. To identify the most plausible explanations, existing work has primarily relied on surrogate models to learn how the input data is distributed. This effectively reallocates the task of learning realistic representations of the data from the model itself to the surrogate. Consequently, the generated explanations may look plausible to humans but not necessarily faithfully describe the behaviour of the black-box model. We formalise this notion of faithfulness through the introduction of a tailored evaluation metric and propose a novel algorithmic framework for generating **Energy-Constrained Conformal Counterfactuals** that are only as plausible as the model permits. Through extensive empirical studies involving multiple synthetic and real-world datasets, we demonstrate that ECCCoS reconcile the need for plausibility and faithfulness. In particular, we show that it is possible to achieve state-of-the-art plausibility for any black-box model with gradient access without the need for surrogate models. To do so, **ECCCo** relies solely on properties defining the black-box model itself by leveraging recent advances in energy-based modelling and conformal inference. The empirical findings also highlight that black-box models that are trained jointly to discriminate outputs and generate inputs tend to yield more plausible explanations than pure discriminative models. Our framework is intuitive, flexible and open-sourced. By highlighting the need for faithfulness in the context of Counterfactual Explanations, we believe that in the short term, our work will enable researchers and practitioners to better distinguish trustworthy from unreliable models. We anticipate that ECCCo can serve as a baseline for future research directed at providing plausible but faithful Counterfactual Explanations.

1 Introduction

Counterfactual Explanations provide a powerful, flexible and intuitive way to not only explain black-box models but also enable affected individuals to challenge them through the means of Algorithmic Recourse. Instead of opening the black box, Counterfactual Explanations work under the premise of strategically perturbing model inputs to understand model behaviour [29]. Intuitively speaking, we generate explanations in this context by asking simple what-if questions of the following nature: ‘Our credit risk model currently predicts that this individual’s credit profile is too risky to offer them a loan. What if they reduced their monthly expenditures by 10%? Will our model then predict that the individual is credit-worthy?’

This is typically implemented by defining a target outcome $\mathbf{y}^* \in \mathcal{Y}$ for some individual $\mathbf{x} \in \mathcal{X} = \mathbb{R}^D$ described by D attributes, for which the model $M_\theta : \mathcal{X} \mapsto \mathcal{Y}$ initially predicts a different outcome:

36 $M_\theta(\mathbf{x}) \neq \mathbf{y}^*$. Counterfactuals are then searched by minimizing a loss function that compares the
 37 predicted model output to the target outcome: $\text{yloss}(M_\theta(\mathbf{x}), \mathbf{y}^*)$. Since Counterfactual Explanations
 38 (CE) work directly with the black-box model, valid counterfactuals always have full local fidelity by
 39 construction [17]. Fidelity is defined as the degree to which explanations approximate the predictions
 40 of the black-box model. This is arguably one of the most important evaluation metrics for model
 41 explanations, since any explanation that explains a prediction not actually made by the model is
 42 useless [16].

43 In situations where full fidelity is a requirement, CE therefore offers a more appropriate solution
 44 to Explainable Artificial Intelligence (XAI) than other popular approaches like LIME [22] and
 45 SHAP [12], which involve local surrogate models. But even full fidelity is not a sufficient condition
 46 for ensuring that an explanation faithfully describes the behaviour of a model. That is because
 47 multiple very distinct explanations can all lead to the same model prediction, especially when dealing
 48 with heavily parameterized models like deep neural networks which are typically underspecified by
 49 the available data [30].

50 In the context of CE, the idea that no two explanations are the same arises almost naturally. A key
 51 focus in the literature has therefore been to identify those explanations and algorithmic recourses
 52 that are deemed most appropriate based on a myriad of desiderata such as sparsity, actionability
 53 and plausibility. In this work, we draw closer attention to the insufficiency of model fidelity as an
 54 evaluation metric for the faithfulness of counterfactual explanations. Our key contributions are as
 55 follows: firstly, we introduce a new notion of faithfulness that is suitable for counterfactuals and
 56 propose a novel evaluation measure that draws inspiration from recent advances in Energy-Based
 57 Modelling (EBM); secondly, we a novel algorithmic approach for generating Energy-Constrained
 58 Conformal Counterfactuals (ECCCo) that explicitly address the need for faithfulness; finally, we
 59 provide illustrative examples and extensive empirical evidence demonstrating that ECCCos faithfully
 60 explain model behaviour without sacrificing existing desiderata like plausibility and sparsity.

61 2 Background and Related Work

62 In this section, we provide some background on Counterfactual Explanations and our motivation for
 63 this work. To start, we briefly introduce the methodology underlying most state-of-the-art (SOTA)
 64 counterfactual generators.

65 2.1 Gradient-Based Counterfactual Search

66 While Counterfactual Explanations can be generated for arbitrary regression models [24], existing
 67 work has primarily focused on classification problems. Let $\mathcal{Y} = (0, 1)^K$ denote the one-hot-encoded
 68 output domain with K classes. Then most SOTA counterfactual generators rely on gradient descent
 69 to optimize different flavours of the following counterfactual search objective:

$$\mathbf{Z}' = \arg \min_{\mathbf{Z}' \in \mathcal{Z}^L} \{\text{yloss}(M_\theta(f(\mathbf{Z}')), \mathbf{y}^*) + \lambda \text{cost}(f(\mathbf{Z}'))\} \quad (1)$$

70 Here yloss denotes the primary loss function already introduced above and cost is either a single
 71 penalty or a collection of penalties that are used to impose constraints through regularization. Equa-
 72 tion 1 restates the baseline approach to gradient-based counterfactual search proposed by Wachter
 73 et al. [29] in general form where $\mathbf{Z}' = \{\mathbf{z}_l\}_L$ denotes an L -dimensional array of counterfactual
 74 states [2]. This is to explicitly account for the multiplicity of explanations and the fact that we may
 75 choose to generate multiple counterfactuals and traverse a latent encoding \mathcal{Z} of the feature space \mathcal{X}
 76 where we denote $f^{-1} : \mathcal{X} \mapsto \mathcal{Z}$. Encodings may involve simple feature transformations or more
 77 advanced techniques involving generative models, as we will discuss further below. The baseline
 78 approach, which we will simply refer to as **Wachter** [29], searches a single counterfactual directly in
 79 the feature space and penalises its distance between the original factual.

80 Solutions to Equation 1 are considered valid as soon as the predicted label matches the target label. A
 81 stripped-down counterfactual explanation is therefore little different from an adversarial example. In
 82 Figure 1, for example, we have applied Wachter to MNIST data (centre panel) where the underlying
 83 classifier M_θ is a simple Multi-Layer Perceptron (MLP) with above 90 percent test accuracy. For the
 84 generated counterfactual \mathbf{x}' the model predicts the target label with high confidence (centre panel

in Figure 1). The explanation is valid by definition, even though it looks a lot like an Adversarial Example [6]. Schut et al. [23] make the connection between Adversarial Examples and Counterfactual Explanations explicit and propose using a Jacobian-Based Saliency Map Attack (JSMA) to solve Equation 1. They demonstrate that this approach yields realistic and sparse counterfactuals for Bayesian, adversarially robust classifiers. Applying their approach to our simple MNIST classifier does not yield a realistic counterfactual but this one, too, is valid (right panel in Figure 1).

2.2 From Adversarial Examples to Plausible Explanations

The crucial difference between Adversarial Examples (AE) and Counterfactual Explanations is one of intent. While an AE is intended to go unnoticed, a CE should have certain desirable properties. The literature has made this explicit by introducing various so-called *desiderata* that counterfactuals should meet in order to properly serve both AI practitioners and individuals affected by AI decision-making systems. The list of desiderata includes but is not limited to the following: sparsity, proximity [29], actionability [27], diversity [17], plausibility [9, 21, 23], robustness [26, 20, 2] and causality [11].

Researchers have come up with various ways to meet these desiderata, which have been extensively surveyed and evaluated in various studies [28, 10, 19, 4, 8]. Perhaps unsurprisingly, the different desiderata are often positively correlated. For example, Artelt et al. [4] find that plausibility typically also leads to improved robustness. Similarly, plausibility has also been connected to causality in the sense that plausible counterfactuals respect causal relationships [13].

2.2.1 Plausibility through Surrogates

Arguably, the plausibility of counterfactuals has been among the primary concerns and some have focused explicitly on this goal. Joshi et al. [9], for example, were among the first to suggest that instead of searching counterfactuals in the feature space \mathcal{X} , we can instead traverse a latent embedding \mathcal{Z} (Equation 1) that implicitly codifies the data generating process (DGP) of $\mathbf{x} \sim \mathcal{X}$. To learn the latent embedding, they introduce a surrogate model. In particular, they propose to use the latent embedding of a Variational Autoencoder (VAE) trained to generate samples $\mathbf{x}^* \leftarrow \mathcal{G}(\mathbf{z})$ where \mathcal{G} denotes the decoder part of the VAE. Provided the surrogate model is well-trained, their proposed approach —REVISE— can yield compelling counterfactual explanations like the one in the centre panel of Figure 2.

Others have proposed similar approaches. Dombrowski et al. [5] traverse the base space of a normalizing flow to solve Equation 1, essentially relying on a different surrogate model for the generative task. Poyiadzi et al. [21] use density estimators ($\hat{p} : \mathcal{X} \mapsto [0, 1]$) to constrain the counterfactuals to dense regions in the feature space. Karimi et al. [11] argue that counterfactuals should comply with the causal model that generates the data. All of these different approaches share a common goal: ensuring that the generated counterfactuals comply with the true and unobserved DGP. To summarize this broad objective, we propose the following definition:

Definition 2.1 (Plausible Counterfactuals). *Let $\mathcal{X}|\mathbf{y}^*$ denote the true conditional distribution of samples in the target class \mathbf{y}^* . Then for \mathbf{x}' to be considered a plausible counterfactual, we need: $\mathbf{x}' \sim \mathcal{X}|\mathbf{y}^*$.*

Surrogate models offer an obvious solution to achieve this objective. Unfortunately, surrogates also introduce a dependency: the generated explanations no longer depend exclusively on the black-box model itself, but also on the surrogate model. This is not necessarily problematic if the primary objective is not to explain the behaviour of the model but to offer recourse to individuals affected by it. It may become problematic even in this context if the dependency turns into a vulnerability. To illustrate this point, we have used REVISE [9] with an underfitted VAE to generate the counterfactual in the right panel of Figure 2: in this case, the decoder step of the VAE fails to yield plausible values ($\{\mathbf{x}' \leftarrow \mathcal{G}(\mathbf{z})\} \not\sim \mathcal{X}|\mathbf{y}^*$) and hence the counterfactual search in the learned latent space is doomed.

2.2.2 Plausibility through Minimal Predictive Uncertainty

Schut et al. [23] show that to meet the plausibility objective we need not explicitly model the input distribution. Pointing to the undesirable engineering overhead induced by surrogate models, they propose that we rely on the implicit minimisation of predictive uncertainty instead. Their proposed methodology solves Equation 1 by greedily applying JSMA in the feature space with standard cross-entropy loss and no penalty at all. They demonstrate theoretically and empirically that their approach

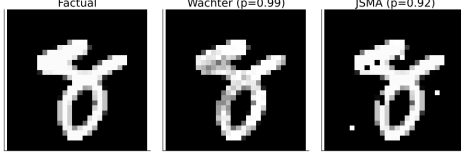


Figure 1: Explanations or Adversarial Examples? Counterfactuals for turning an 8 (eight) into a 3 (three): original image (left); counterfactual produced using Wachter et al. [29] (centre); and a counterfactual produced using the approach introduced by [23] that uses Jacobian-Based Saliency Map Attacks to solve Equation 1.

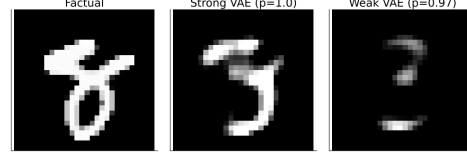


Figure 2: Using surrogates can improve plausibility, but also increases vulnerability. Counterfactuals for turning an 8 (eight) into a 3 (three): original image (left); counterfactual produced using REVISE [9] with a well-specified surrogate (centre); and a counterfactual produced using REVISE [9] with a poorly specified surrogate (right).

137 yields counterfactuals for which the model M_θ predicts the target label \mathbf{y}^* with high confidence.
 138 Provided the model is well-specified, these counterfactuals are plausible. Unfortunately, this idea
 139 hinges on the assumption that the black-box model provides well-calibrated predictive uncertainty
 140 estimates.

141 2.3 From Fidelity to Model Conformity

142 Above we explained that since Counterfactual Explanations work directly with the Black Box model,
 143 the fidelity of explanations as we defined it earlier is not a concern. This may explain why research has
 144 primarily focused on other desiderata, most notably plausibility (Definition 2.1). Enquiring about the
 145 plausibility of a counterfactual essentially boils down to the following question: ‘Is this counterfactual
 146 consistent with the underlying data?’ We posit a related, slightly more nuanced question: ‘Is this
 147 counterfactual consistent with what the model has learned about the underlying data?’ We will argue
 148 that fidelity is not a sufficient evaluation measure to answer this question and propose a novel way to
 149 assess if Counterfactual Explanations conform with model behaviour.

150 The word *fidelity* stems from the Latin word ‘fidelis’, which means ‘faithful, loyal, trustworthy’ [15].
 151 As we explained in Section 2, model explanations are generally considered faithful if their corre-
 152 sponding predictions coincide with the predictions made by the model itself. Since this definition
 153 of faithfulness is not useful in the context of Counterfactual Explanations, we propose an adapted
 154 version:

155 **Definition 2.2** (Conformal Counterfactuals). *Let $\mathcal{X}_\theta|\mathbf{y}^* = p_\theta(x|\mathbf{y}^*)$ denote the conditional distri-*
 156 *bution of \mathbf{x} in the target class \mathbf{y}^* , where θ denotes the parameters of model M_θ . Then for \mathbf{x}' to be*
 157 *considered a conformal counterfactual, we need: $\mathbf{x}' \sim \mathcal{X}_\theta|\mathbf{y}^*$.*

158 In words, conformal counterfactuals conform with what the predictive model has learned about
 159 the input data \mathbf{x} . Since this definition works with distributional properties, it explicitly accounts
 160 for the multiplicity of explanations we discussed earlier. To assess counterfactuals with respect to
 161 Definition 2.2, we need to be able to quantify the posterior conditional distribution $p_\theta(\mathbf{x}|\mathbf{y}^*)$. This is
 162 very much at the core of our proposed methodological framework, which reconciles the notions of
 163 plausibility and model conformity and which we will introduce next.

164 3 Methodological Framework

165 The primary objective of this work has been to develop a methodology for generating maximally
 166 plausible counterfactuals under minimal intervention. Our proposed framework is based on the
 167 premise that explanations should be plausible but not plausible at all costs. Energy-Constrained
 168 Conformal Counterfactuals (ECCCo) achieve this goal in two ways: firstly, they rely on the Black
 169 Box itself for the generative task; and, secondly, they involve an approach to predictive uncertainty
 170 quantification that is model-agnostic.

3.1 Quantifying the Model’s Generative Property

Recent work by Grathwohl et al. [7] on Energy Based Models (EBM) has pointed out that there is a ‘generative model hidden within every standard discriminative model’. The authors show that we can draw samples from the posterior conditional distribution $p_\theta(\mathbf{x}|\mathbf{y})$ using Stochastic Gradient Langevin Dynamics (SGLD). The authors use this insight to train classifiers jointly for the discriminative task using standard cross-entropy and the generative task using SGLD. They demonstrate empirically that among other things this improves predictive uncertainty quantification for discriminative models. Our findings in this work suggest that Joint Energy Models (JEM) also tend to yield more plausible Counterfactual Explanations. Based on the definition of plausible counterfactuals (Definition 2.1) this is not surprising.

Crucially for our purpose, one can apply their proposed sampling strategy during inference to essentially any standard discriminative model. Even models that are not explicitly trained for the joint objective learn about the distribution of inputs X by learning to make conditional predictions about the output y . We can leverage this observation to quantify the generative property of the Black Box model itself. In particular, note that if we fix \mathbf{y} to our target value \mathbf{y}^* , we can sample from $p_\theta(\mathbf{x}|\mathbf{y}^*)$ using SGLD as follows,

$$\mathbf{x}_{j+1} \leftarrow \mathbf{x}_j - \frac{\epsilon^2}{2} \mathcal{E}(\mathbf{x}_j|\mathbf{y}^*) + \epsilon \mathbf{r}_j, \quad j = 1, \dots, J \quad (2)$$

where $\mathbf{r}_j \sim \mathcal{N}(\mathbf{0}, \mathbf{I})$ is the stochastic term and the step-size ϵ is typically polynomially decayed. The term $\mathcal{E}(\mathbf{x}_j|\mathbf{y}^*)$ denotes the energy function where we use $\mathcal{E}(\mathbf{x}_j|\mathbf{y}^*) = -M_\theta(\mathbf{x}_j)[\mathbf{y}^*]$, that is the negative logit corresponding to the target class label \mathbf{y}^* . Generating multiple samples in this manner yields an empirical distribution $\hat{\mathcal{X}}_\theta|\mathbf{y}^*$ that we use in our search for plausible counterfactuals, as discussed in more detail below. Appendix A provides additional implementation details for any tasks related to energy-based modelling.

3.2 Quantifying the Model’s Predictive Uncertainty

To quantify the model’s predictive uncertainty we use Conformal Prediction (CP), an approach that has recently gained popularity in the Machine Learning community [3, 14]. Crucially for our intended application, CP is model-agnostic and can be applied during inference without placing any restrictions on model training. Intuitively, CP works under the premise of turning heuristic notions of uncertainty into rigorous uncertainty estimates by repeatedly sifting through the training data or a dedicated calibration dataset. Conformal classifiers produce prediction sets for individual inputs that include all output labels that can be reasonably attributed to the input. These sets tend to be larger for inputs that do not conform with the training data and are therefore characterized by high predictive uncertainty.

In order to generate counterfactuals that are associated with low predictive uncertainty, we use a smooth set size penalty introduced by Stutz et al. [25] in the context of conformal training:

$$\Omega(C_\theta(\mathbf{x}; \alpha)) = \max \left(0, \sum_{\mathbf{y} \in \mathcal{Y}} C_{\theta, \mathbf{y}}(\mathbf{x}_i; \alpha) - \kappa \right) \quad (3)$$

Here, $\kappa \in \{0, 1\}$ is a hyper-parameter and $C_{\theta, \mathbf{y}}(\mathbf{x}_i; \alpha)$ can be interpreted as the probability of label \mathbf{y} being included in the prediction set.

In order to compute this penalty for any black-box model we merely need to perform a single calibration pass through a holdout set \mathcal{D}_{cal} . Arguably, data is typically abundant and in most applications, practitioners tend to hold out a test data set anyway. Consequently, CP removes the restriction on the family of predictive models, at the small cost of reserving a subset of the available data for calibration. This particular case of conformal prediction is referred to as Split Conformal Prediction (SCP) as it involves splitting the training data into a proper training dataset and a calibration dataset. Details concerning our implementation of Conformal Prediction can be found in Appendix B.

3.3 Energy-Constrained Conformal Counterfactuals (ECCCo)

Our framework for generating ECCCos combines the ideas introduced in the previous two subsections. Formally, we extend Equation 1 as follows,

$$\mathbf{Z}' = \arg \min_{\mathbf{Z}' \in \mathcal{Z}^M} \{ \text{yloss}(M_\theta(f(\mathbf{Z}')), \mathbf{y}^*) + \lambda_1 \text{dist}(f(\mathbf{Z}'), \mathbf{x}) + \lambda_2 \text{dist}(f(\mathbf{Z}'), \hat{\mathbf{x}}_\theta) + \lambda_3 \Omega(C_\theta(f(\mathbf{Z}'); \alpha)) \} \quad (4)$$

where $\hat{\mathbf{x}}_\theta$ denotes samples generated using SGLD (Equation 2) and $\text{dist}(\cdot)$ is a generic term for a distance metric. Our default choice for $\text{dist}(\cdot)$ is the L1 Norm, or Manhattan distance, since it induces sparsity.

The first two terms in Equation 4 correspond to the counterfactual search objective defined in Wachter et al. [29] which merely penalises the distance of counterfactuals from their factual values. The additional two penalties in ECCCo ensure that counterfactuals conform with the model’s generative property and lead to minimally uncertain predictions, respectively. The hyperparameters $\lambda_1, \dots, \lambda_3$ can be used to balance the different objectives: for example, we may choose to incur larger deviations from the factual in favour of conformity with the model’s generative property by choosing lower values of λ_1 and relatively higher values of λ_2 . Figure 3 illustrates this balancing act for an example involving synthetic data: vector fields indicate the direction of gradients with respect to the different components our proposed objective function (Equation 4).

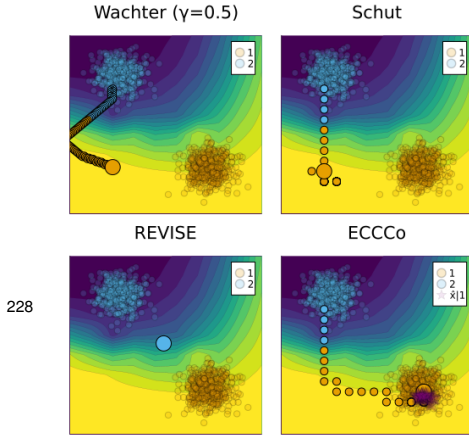


Figure 3: [PLACEHOLDER] Vector fields indicating the direction of gradients with respect to the different components of the ECCCo objective (Equation 4).

Algorithm 1: Generating ECCCos (For more details, see Appendix C)

Input: $\mathbf{x}, \mathbf{y}^*, M_\theta, f, \Lambda, \alpha, \mathcal{D}, T, \eta, n_B, N_B$
where $M_\theta(\mathbf{x}) \neq \mathbf{y}^*$
Output: \mathbf{x}'
1: Initialize $\mathbf{z}' \leftarrow f^{-1}(\mathbf{x})$
2: Generate buffer \mathcal{B} of N_B conditional samples $\hat{\mathbf{x}}_\theta | \mathbf{y}^*$ using SGLD (Equation 2)
3: Run SCP for M_θ using \mathcal{D}
4: Initialize $t \leftarrow 0$
5: **while** not converged or $t < T$ **do**
6: $\hat{\mathbf{x}}_{\theta,t} \leftarrow \text{rand}(\mathcal{B}, n_B)$
7: $\mathbf{z}' \leftarrow \mathbf{z}' - \eta \nabla_{\mathbf{z}'} \mathcal{L}(\mathbf{z}', \mathbf{y}^*, \hat{\mathbf{x}}_{\theta,t}; \Lambda, \alpha)$
8: $t \leftarrow t + 1$
9: **end while**
10: $\mathbf{x}' \leftarrow f(\mathbf{z}')$

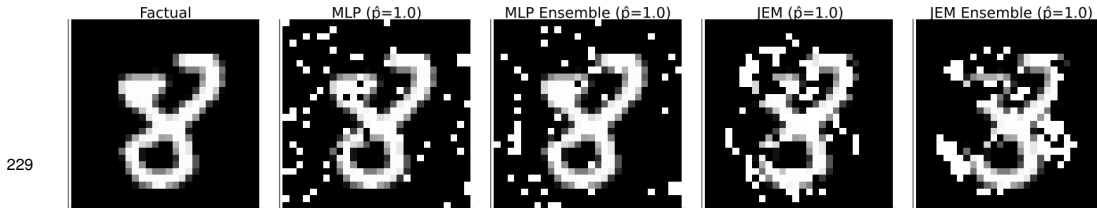


Figure 4: [SUBJECT TO CHANGE] Original image (left) and ECCCos for turning an 8 (eight) into a 3 (three) for different Black Boxes from left to right: Multi-Layer Perceptron (MLP), Ensemble of MLPs, Joint Energy Model (JEM), Ensemble of JEMs.

The entire procedure for Generating ECCCos is described in Algorithm 1. For the sake of simplicity and without loss of generality, we limit our attention to generating a single counterfactual $\mathbf{x}' = f(\mathbf{z}')$ where in contrast to Equation 4 \mathbf{z}' denotes a 1-dimensional array containing a single counterfactual

state. That state is initialized by passing the factual \mathbf{x} through the encoder f^{-1} which in our case corresponds to a simple feature transformer, rather than the encoder part of VAE as in REVISE [9]. Next, we generate a buffer of N_B conditional samples $\hat{\mathbf{x}}_\theta|\mathbf{y}^*$ using SGLD (Equation 2) and conformalise the model M_θ through Split Conformal Prediction on training data \mathcal{D} .

Finally, we search counterfactuals through gradient descent. Let $\mathcal{L}(\mathbf{z}', \mathbf{y}^*, \hat{\mathbf{x}}_{\theta,t}; \Lambda, \alpha)$ denote our loss function defined in Equation 4. Then in each iteration, we first randomly draw n_B samples from the buffer \mathcal{B} before updating the counterfactual state \mathbf{z}' by moving in the negative direction of that loss function. The search terminates once the convergence criterium is met or the maximum number of iterations T has been exhausted. Note that the choice of convergence criterium has important implications on the final counterfactual (for more detail on this see Appendix C).

Figure 4 presents ECCCos for the MNIST example from Section 2 for various black-box models of increasing complexity from left to right: a simple Multi-Layer Perceptron (MLP); an Ensemble of MLPs, each of the same architecture as the single MLP; a Joint Energy Model (JEM) based on the same MLP architecture; and finally, an Ensemble of these JEMs. Since Deep Ensembles have an improved capacity for predictive uncertainty quantification and JEMs are explicitly trained to learn plausible representations of the input data, it is intuitive to see that the plausibility of counterfactuals visibly improves from left to right. This provides some first anecdotal evidence that ECCCos achieve plausibility while maintaining faithfulness to the Black Box.

4 Empirical Analysis

In this section, we bolster our anecdotal findings from the previous section through rigorous empirical analysis. We first briefly describe our evaluation framework and data, before presenting and discussing our results.

4.1 Evaluation Measures

Above we have defined plausibility (Definition 2.1) and conformity (Definition 2.2) for Counterfactual Explanations. In this subsection, we introduce evaluation measures that facilitate a quantitative evaluation of counterfactuals for these objectives.

Firstly, in order to assess the plausibility of counterfactuals we adapt the implausibility metric proposed in Guidotti [8]. The authors propose to evaluate plausibility in terms of the distance of the counterfactual \mathbf{x}' from its nearest neighbour in the target class \mathbf{y}^* : the smaller this distance, the more plausible the counterfactual. Instead of focusing only on the nearest neighbour of \mathbf{x}' , we suggest computing the average over distances from multiple (possibly all) observed instances in the target class. Formally, for a single counterfactual, we have:

$$\text{impl} = \frac{1}{|\mathbf{x} \in \mathcal{X}|\mathbf{y}^*|} \sum_{\mathbf{x} \in \mathcal{X}|\mathbf{y}^*} \text{dist}(\mathbf{x}', \mathbf{x}) \quad (5)$$

This measure is straightforward to compute and should be less sensitive to outliers in the target class than the one based on the nearest neighbour. It also gives rise to a very similar evaluation measure for conformity. We merely swap out the subsample of individuals in the target class for the empirical distribution of generated conditional samples:

$$\text{conf} = \frac{1}{|\mathbf{x} \in \mathcal{X}_\theta|\mathbf{y}^*|} \sum_{\mathbf{x} \in \mathcal{X}_\theta|\mathbf{y}^*} \text{dist}(\mathbf{x}', \mathbf{x}) \quad (6)$$

As noted by Guidotti [8], these distance-based measures are simplistic and more complex alternative measures may ultimately be more appropriate for the task. For example, we considered using statistical divergence measures instead. This would involve generating not one but many counterfactuals and comparing the generated empirical distribution to the target distributions in Definitions 2.1 and 2.2. While this approach is potentially more rigorous, generating enough counterfactuals is not always practical.

Table 1: Results for synthetic datasets. Standard deviation in parentheses.

Model	Generator	Moons	
		Non-conformity ↓	Implausibility ↓
JEM	ECCCo	0.10 (0.03)	1.01 (0.24)
	REVISE	0.64 (0.34)	1.12 (0.51)
	Schut	0.54 (0.38)	1.10 (0.37)
	Wachter	0.74 (0.36)	1.38 (0.38)
MLP	ECCCo	0.20 (0.36)	1.45 (0.86)
	REVISE	0.38 (0.39)	1.10 (0.51)
	Schut	0.73 (0.53)	1.26 (0.67)
	Wachter	0.78 (0.52)	1.33 (0.60)

Table 2: Results for real-world datasets. Standard deviation in parentheses.

Model	Generator	California Housing		GMSC		MNIST	
		Non-conformity ↓	Implausibility ↓	Non-conformity ↓	Implausibility ↓	Non-conformity ↓	Implausibility ↓
JEM	ECCCo	4.31 (0.58)	5.37 (0.46)	3.14 (0.31)	5.34 (1.27)	99.01 (12.50)	120.76 (9.23)
	REVISE	5.01 (0.59)	5.33 (0.58)	2.86 (0.17)	3.99 (0.44)	101.01 (15.20)	115.14 (20.10)
	Schut	5.23 (0.74)	6.50 (0.84)	3.43 (0.53)	5.29 (1.27)	179.39 (29.17)	190.01 (34.50)
	Wachter	5.29 (0.52)	6.48 (0.70)	3.40 (0.38)	5.50 (1.35)	197.35 (32.89)	199.65 (35.60)
JEM Ensemble	ECCCo	3.51 (0.62)	5.33 (0.53)	3.01 (0.76)	6.09 (1.01)	85.30 (14.79)	102.27 (4.72)
	REVISE	4.33 (0.38)	4.73 (0.22)	2.21 (0.72)	4.53 (0.86)	119.87 (16.20)	110.30 (12.11)
	Schut	5.81 (0.61)	6.53 (0.81)	3.10 (0.75)	6.06 (1.01)	171.19 (22.13)	178.31 (24.94)
	Wachter	5.02 (0.85)	6.07 (1.04)	2.89 (0.76)	5.87 (0.88)	222.18 (23.50)	212.40 (27.99)
MLP	ECCCo	145.15 (28.83)	8.84 (1.01)	38.28 (3.68)	5.14 (0.87)	416.59 (14.69)	204.16 (24.95)
	REVISE	119.53 (11.72)	5.28 (0.97)	40.31 (3.38)	3.94 (0.86)	444.47 (10.01)	95.53 (13.46)
	Schut	151.20 (28.78)	7.04 (1.27)	35.73 (6.30)	5.12 (0.85)	477.40 (17.45)	197.85 (25.43)
	Wachter	131.81 (40.19)	6.81 (1.22)	36.70 (14.79)	5.28 (0.87)	444.82 (13.20)	198.27 (24.73)
MLP Ensemble	ECCCo	125.55 (22.76)	10.06 (1.40)	34.32 (4.47)	5.09 (1.20)	397.02 (7.99)	214.01 (21.17)
	REVISE	151.49 (20.56)	6.17 (1.83)	35.26 (4.48)	4.15 (0.72)	430.37 (10.51)	95.87 (7.51)
	Schut	106.34 (30.66)	8.49 (2.22)	30.44 (6.35)	5.15 (1.18)	471.16 (7.93)	203.43 (19.51)
	Wachter	152.35 (21.75)	7.68 (1.89)	36.15 (8.28)	5.03 (0.78)	421.75 (9.75)	206.04 (20.35)

4.2 Data

4.3 Results

See Table 2

5 Discussion

5.1 Key Insights

Consistent with the findings in Schut et al. [23], we have demonstrated that predictive uncertainty estimates can be leveraged to generate plausible counterfactuals. Interestingly, Schut et al. [23] point out that this finding — as intuitive as it is — may be linked to a positive connection between the generative task and predictive uncertainty quantification. In particular, Grathwohl et al. [7] demonstrate that their proposed method for integrating the generative objective in training yields models that have improved predictive uncertainty quantification. Since neither Schut et al. [23] nor we have employed any surrogate generative models, our findings seem to indicate that the positive connection found in Grathwohl et al. [7] is bidirectional.

5.2 Limitations

- BatchNorm does not seem compatible with JEM
- Coverage and temperature impacts CCE in somewhat unpredictable ways
- It seems that models that are not explicitly trained for generative task, still learn it implicitly
- Batch size seems to impact quality of generated samples (at inference, but not so much during JEM training)

- ECCCo is sensitive to optimizer (Adam works well), learning rate and distance metric (11 currently only one that works)
- SGLD takes time
- REVISE has benefit of lower dimensional space
- For MNIST it seems that ECCCo is better at reducing pixel values than increasing them (better at erasing than writing)
- JEMs are more difficult to train

6 Conclusion

References

- [1] Patrick Altmeyer. Conformal Prediction in Julia. URL <https://www.paltmeyer.com/blog/posts/conformal-prediction/>.
- [2] Patrick Altmeyer, Giovan Angela, Aleksander Buszydluk, Karol Dobiczek, Arie van Deursen, and Cynthia Liem. Endogenous Macrodynamics in Algorithmic Recourse. In *First IEEE Conference on Secure and Trustworthy Machine Learning*, 2023.
- [3] Anastasios N. Angelopoulos and Stephen Bates. A gentle introduction to conformal prediction and distribution-free uncertainty quantification. 2021.
- [4] André Artelt, Valerie Vaquet, Riza Velioglu, Fabian Hinder, Johannes Brinkrolf, Malte Schilling, and Barbara Hammer. Evaluating Robustness of Counterfactual Explanations. Technical report, arXiv. URL <http://arxiv.org/abs/2103.02354>. arXiv:2103.02354 [cs] type: article.
- [5] Ann-Kathrin Dombrowski, Jan E Gerken, and Pan Kessel. Diffeomorphic explanations with normalizing flows. In *ICML Workshop on Invertible Neural Networks, Normalizing Flows, and Explicit Likelihood Models*, 2021.
- [6] Ian J Goodfellow, Jonathon Shlens, and Christian Szegedy. Explaining and harnessing adversarial examples. 2014.
- [7] Will Grathwohl, Kuan-Chieh Wang, Joern-Henrik Jacobsen, David Duvenaud, Mohammad Norouzi, and Kevin Swersky. Your classifier is secretly an energy based model and you should treat it like one. March 2020. URL <https://openreview.net/forum?id=HkxzxONtDB>.
- [8] Riccardo Guidotti. Counterfactual explanations and how to find them: literature review and benchmarking. ISSN 1573-756X. doi: 10.1007/s10618-022-00831-6. URL <https://doi.org/10.1007/s10618-022-00831-6>.
- [9] Shalmali Joshi, Oluwasanmi Koyejo, Warut Vijitbenjaronk, Been Kim, and Joydeep Ghosh. Towards realistic individual recourse and actionable explanations in black-box decision making systems. 2019.
- [10] Amir-Hossein Karimi, Gilles Barthe, Bernhard Schölkopf, and Isabel Valera. A survey of algorithmic recourse: Definitions, formulations, solutions, and prospects. 2020.
- [11] Amir-Hossein Karimi, Bernhard Schölkopf, and Isabel Valera. Algorithmic recourse: From counterfactual explanations to interventions. In *Proceedings of the 2021 ACM Conference on Fairness, Accountability, and Transparency*, pages 353–362, 2021.
- [12] Scott M Lundberg and Su-In Lee. A unified approach to interpreting model predictions. In *Proceedings of the 31st International Conference on Neural Information Processing Systems*, pages 4768–4777, 2017.
- [13] Divyat Mahajan, Chenhao Tan, and Amit Sharma. Preserving Causal Constraints in Counterfactual Explanations for Machine Learning Classifiers. Technical report, arXiv. URL <http://arxiv.org/abs/1912.03277>. arXiv:1912.03277 [cs, stat] type: article.
- [14] Valery Manokhin. Awesome conformal prediction.

- [15] Merriam-Webster. "fidelity". URL <https://www.merriam-webster.com/dictionary/fidelity>.
- [16] Christoph Molnar. *Interpretable Machine Learning*. Lulu. com, 2020.
- [17] Ramaravind K Mothilal, Amit Sharma, and Chenhao Tan. Explaining machine learning classifiers through diverse counterfactual explanations. In *Proceedings of the 2020 Conference on Fairness, Accountability, and Transparency*, pages 607–617, 2020.
- [18] Kevin P. Murphy. *Probabilistic machine learning: Advanced topics*. MIT Press.
- [19] Martin Pawelczyk, Sascha Bielawski, Johannes van den Heuvel, Tobias Richter, and Gjergji Kasneci. Carla: A python library to benchmark algorithmic recourse and counterfactual explanation algorithms. 2021.
- [20] Martin Pawelczyk, Teresa Datta, Johannes van-den Heuvel, Gjergji Kasneci, and Himabindu Lakkaraju. Probabilistically Robust Recourse: Navigating the Trade-offs between Costs and Robustness in Algorithmic Recourse. *arXiv preprint arXiv:2203.06768*, 2022.
- [21] Rafael Poyiadzi, Kacper Sokol, Raul Santos-Rodriguez, Tijl De Bie, and Peter Flach. FACE: Feasible and actionable counterfactual explanations. In *Proceedings of the AAAI/ACM Conference on AI, Ethics, and Society*, pages 344–350, 2020.
- [22] Marco Tulio Ribeiro, Sameer Singh, and Carlos Guestrin. "Why should i trust you?" Explaining the predictions of any classifier. In *Proceedings of the 22nd ACM SIGKDD International Conference on Knowledge Discovery and Data Mining*, pages 1135–1144, 2016.
- [23] Lisa Schut, Oscar Key, Rory Mc Grath, Luca Costabello, Bogdan Sacaleanu, Yarin Gal, et al. Generating Interpretable Counterfactual Explanations By Implicit Minimisation of Epistemic and Aleatoric Uncertainties. In *International Conference on Artificial Intelligence and Statistics*, pages 1756–1764. PMLR, 2021.
- [24] Thomas Spooner, Danial Dervovic, Jason Long, Jon Shepard, Jiahao Chen, and Daniele Magazzini. Counterfactual Explanations for Arbitrary Regression Models. 2021.
- [25] David Stutz, Krishnamurthy Dj Dvijotham, Ali Taylan Cemgil, and Arnaud Doucet. Learning Optimal Conformal Classifiers. May 2022. URL <https://openreview.net/forum?id=t80-4LKfVx>.
- [26] Sohini Upadhyay, Shalmali Joshi, and Himabindu Lakkaraju. Towards Robust and Reliable Algorithmic Recourse. 2021.
- [27] Berk Ustun, Alexander Spangher, and Yang Liu. Actionable recourse in linear classification. In *Proceedings of the Conference on Fairness, Accountability, and Transparency*, pages 10–19, 2019.
- [28] Sahil Verma, John Dickerson, and Keegan Hines. Counterfactual explanations for machine learning: A review. 2020.
- [29] Sandra Wachter, Brent Mittelstadt, and Chris Russell. Counterfactual explanations without opening the black box: Automated decisions and the GDPR. *Harv. JL & Tech.*, 31:841, 2017.
- [30] Andrew Gordon Wilson. The case for Bayesian deep learning. 2020.

Appendices

A JEM

While \mathbf{x}_J is only guaranteed to distribute as $p_\theta(\mathbf{x}|\mathbf{y}^*)$ if $\epsilon \rightarrow 0$ and $J \rightarrow \infty$, the bias introduced for a small finite ϵ is negligible in practice [18, 7]. While Grathwohl et al. [7] use Equation 2 during training, we are interested in applying the conditional sampling procedure in a post-hoc fashion to any standard discriminative model.

383 B Conformal Prediction

384 The fact that conformal classifiers produce set-valued predictions introduces a challenge: it is not
 385 immediately obvious how to use such classifiers in the context of gradient-based counterfactual
 386 search. Put differently, it is not clear how to use prediction sets in Equation 1. Fortunately, Stutz et al.
 387 [25] have recently proposed a framework for Conformal Training that also hinges on differentiability.
 388 Specifically, they show how Stochastic Gradient Descent can be used to train classifiers not only
 389 for the discriminative task but also for additional objectives related to Conformal Prediction. One
 390 such objective is *efficiency*: for a given target error rate α , the efficiency of a conformal classifier
 391 improves as its average prediction set size decreases. To this end, the authors introduce a smooth set
 392 size penalty defined in Equation 3 in the body of this paper

393 Formally, it is defined as $C_{\theta, \mathbf{y}}(\mathbf{x}_i; \alpha) := \sigma((s(\mathbf{x}_i, \mathbf{y}) - \alpha)T^{-1})$ for $\mathbf{y} \in \mathcal{Y}$, where σ is the sigmoid
 394 function and T is a hyper-parameter used for temperature scaling [25].

395 Intuitively, CP works under the premise of turning heuristic notions of uncertainty into rigorous
 396 uncertainty estimates by repeatedly sifting through the data. It can be used to generate prediction
 397 intervals for regression models and prediction sets for classification models [1]. Since the literature
 398 on CE and AR is typically concerned with classification problems, we focus on the latter. A particular
 399 variant of CP called Split Conformal Prediction (SCP) is well-suited for our purposes, because it
 400 imposes only minimal restrictions on model training.

401 Specifically, SCP involves splitting the data $\mathcal{D}_n = \{(\mathbf{x}_i, \mathbf{y}_i)\}_{i=1, \dots, n}$ into a proper training set $\mathcal{D}_{\text{train}}$
 402 and a calibration set \mathcal{D}_{cal} . The former is used to train the classifier in any conventional fashion.
 403 The latter is then used to compute so-called nonconformity scores: $\mathcal{S} = \{s(\mathbf{x}_i, \mathbf{y}_i)\}_{i \in \mathcal{D}_{\text{cal}}}$ where
 404 $s : (\mathcal{X}, \mathcal{Y}) \mapsto \mathbb{R}$ is referred to as *score function*. In the context of classification, a common choice for
 405 the score function is just $s_i = 1 - M_{\theta}(\mathbf{x}_i)[\mathbf{y}_i]$, that is one minus the softmax output corresponding
 406 to the observed label \mathbf{y}_i [3].

407 Finally, classification sets are formed as follows,

$$C_{\theta}(\mathbf{x}_i; \alpha) = \{\mathbf{y} : s(\mathbf{x}_i, \mathbf{y}) \leq \hat{q}\} \quad (7)$$

408 where \hat{q} denotes the $(1 - \alpha)$ -quantile of \mathcal{S} and α is a predetermined error rate. As the size of the
 409 calibration set increases, the probability that the classification set $C(\mathbf{x}_{\text{test}})$ for a newly arrived sample
 410 \mathbf{x}_{test} does not cover the true test label \mathbf{y}_{test} approaches α [3].

411 Observe from Equation 7 that Conformal Prediction works on an instance-level basis, much like
 412 Counterfactual Explanations are local. The prediction set for an individual instance \mathbf{x}_i depends only
 413 on the characteristics of that sample and the specified error rate. Intuitively, the set is more likely
 414 to include multiple labels for samples that are difficult to classify, so the set size is indicative of
 415 predictive uncertainty. To see why this effect is exacerbated by small choices for α consider the case
 416 of $\alpha = 0$, which requires that the true label is covered by the prediction set with probability equal to
 417 1.

418 C Conformal Prediction

419 A Submission of papers to NeurIPS 2023

420 Please read the instructions below carefully and follow them faithfully.

421 A Style

422 Papers to be submitted to NeurIPS 2023 must be prepared according to the instructions presented
 423 here. Papers may only be up to **nine** pages long, including figures. Additional pages *containing only*
 424 *acknowledgments and references* are allowed. Papers that exceed the page limit will not be reviewed,
 425 or in any other way considered for presentation at the conference.

426 The margins in 2023 are the same as those in previous years.

427 Authors are required to use the NeurIPS L^AT_EX style files obtainable at the NeurIPS website as
428 indicated below. Please make sure you use the current files and not previous versions. Tweaking the
429 style files may be grounds for rejection.

430 B Retrieval of style files

431 The style files for NeurIPS and other conference information are available on the website at

432 <http://www.neurips.cc/>

433 The file `neurips_2023.pdf` contains these instructions and illustrates the various formatting re-
434 quirements your NeurIPS paper must satisfy.

435 The only supported style file for NeurIPS 2023 is `neurips_2023.sty`, rewritten for L^AT_EX 2_ε.
436 **Previous style files for L^AT_EX 2.09, Microsoft Word, and RTF are no longer supported!**

437 The L^AT_EX style file contains three optional arguments: `final`, which creates a camera-ready copy,
438 `preprint`, which creates a preprint for submission to, e.g., arXiv, and `nonatbib`, which will not
439 load the `natbib` package for you in case of package clash.

440 **Preprint option** If you wish to post a preprint of your work online, e.g., on arXiv, using the
441 NeurIPS style, please use the `preprint` option. This will create a nonanonymized version of your
442 work with the text “Preprint. Work in progress.” in the footer. This version may be distributed as you
443 see fit, as long as you do not say which conference it was submitted to. Please **do not** use the `final`
444 option, which should **only** be used for papers accepted to NeurIPS.

445 At submission time, please omit the `final` and `preprint` options. This will anonymize your
446 submission and add line numbers to aid review. Please do *not* refer to these line numbers in your
447 paper as they will be removed during generation of camera-ready copies.

448 The file `neurips_2023.tex` may be used as a “shell” for writing your paper. All you have to do is
449 replace the author, title, abstract, and text of the paper with your own.

450 The formatting instructions contained in these style files are summarized in Sections B, C, and D
451 below.

452 B General formatting instructions

453 The text must be confined within a rectangle 5.5 inches (33 picas) wide and 9 inches (54 picas) long.
454 The left margin is 1.5 inch (9 picas). Use 10 point type with a vertical spacing (leading) of 11 points.
455 Times New Roman is the preferred typeface throughout, and will be selected for you by default.
456 Paragraphs are separated by 1/2 line space (5.5 points), with no indentation.

457 The paper title should be 17 point, initial caps/lower case, bold, centered between two horizontal
458 rules. The top rule should be 4 points thick and the bottom rule should be 1 point thick. Allow 1/4 inch
459 space above and below the title to rules. All pages should start at 1 inch (6 picas) from the top of the
460 page.

461 For the final version, authors’ names are set in boldface, and each name is centered above the
462 corresponding address. The lead author’s name is to be listed first (left-most), and the co-authors’
463 names (if different address) are set to follow. If there is only one co-author, list both author and
464 co-author side by side.

465 Please pay special attention to the instructions in Section D regarding figures, tables, acknowledg-
466 ments, and references.

467 C Headings: first level

468 All headings should be lower case (except for first word and proper nouns), flush left, and bold.

469 First-level headings should be in 12-point type.

470 **A Headings: second level**

471 Second-level headings should be in 10-point type.

472 **A.1 Headings: third level**

473 Third-level headings should be in 10-point type.

474 **Paragraphs** There is also a `\paragraph` command available, which sets the heading in bold, flush
475 left, and inline with the text, with the heading followed by 1 em of space.

476 **D Citations, figures, tables, references**

477 These instructions apply to everyone.

478 **A Citations within the text**

479 The `natbib` package will be loaded for you by default. Citations may be author/year or numeric, as
480 long as you maintain internal consistency. As to the format of the references themselves, any style is
481 acceptable as long as it is used consistently.

482 The documentation for `natbib` may be found at

483 `http://mirrors.ctan.org/macros/latex/contrib/natbib/natnotes.pdf`

484 Of note is the command `\citet`, which produces citations appropriate for use in inline text. For
485 example,

486 `\citet{hasselmo}` investigated\dots

487 produces

488 Hasselmo, et al. (1995) investigated...

489 If you wish to load the `natbib` package with options, you may add the following before loading the
490 `neurips_2023` package:

491 `\PassOptionsToPackage{options}{natbib}`

492 If `natbib` clashes with another package you load, you can add the optional argument `nonatbib`
493 when loading the style file:

494 `\usepackage[nonatbib]{neurips_2023}`

495 As submission is double blind, refer to your own published work in the third person. That is, use “In
496 the previous work of Jones et al. [4],” not “In our previous work [4].” If you cite your other papers
497 that are not widely available (e.g., a journal paper under review), use anonymous author names in the
498 citation, e.g., an author of the form “A. Anonymous” and include a copy of the anonymized paper in
499 the supplementary material.

500 **B Footnotes**

501 Footnotes should be used sparingly. If you do require a footnote, indicate footnotes with a number¹
502 in the text. Place the footnotes at the bottom of the page on which they appear. Precede the footnote
503 with a horizontal rule of 2 inches (12 picas).

504 Note that footnotes are properly typeset *after* punctuation marks.²

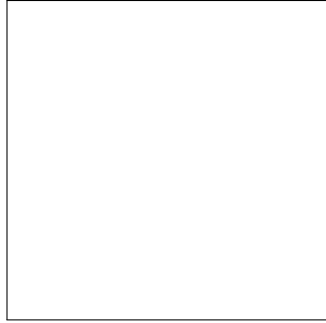


Figure 5: Sample figure caption.

Table 3: Sample table title

Part		
Name	Description	Size (μm)
Dendrite	Input terminal	~ 100
Axon	Output terminal	~ 10
Soma	Cell body	up to 10^6

505 C Figures

506 All artwork must be neat, clean, and legible. Lines should be dark enough for purposes of reproduction.
 507 The figure number and caption always appear after the figure. Place one line space before the figure
 508 caption and one line space after the figure. The figure caption should be lower case (except for first
 509 word and proper nouns); figures are numbered consecutively.

510 You may use color figures. However, it is best for the figure captions and the paper body to be legible
 511 if the paper is printed in either black/white or in color.

512 D Tables

513 All tables must be centered, neat, clean and legible. The table number and title always appear before
 514 the table. See Table 3.

515 Place one line space before the table title, one line space after the table title, and one line space after
 516 the table. The table title must be lower case (except for first word and proper nouns); tables are
 517 numbered consecutively.

518 Note that publication-quality tables *do not contain vertical rules*. We strongly suggest the use of the
 519 booktabs package, which allows for typesetting high-quality, professional tables:

520 <https://www.ctan.org/pkg/booktabs>

521 This package was used to typeset Table 3.

522 E Math

523 Note that display math in bare TeX commands will not create correct line numbers for sub-
 524 mission. Please use LaTeX (or AMSTeX) commands for unnumbered display math. (You
 525 really shouldn't be using \$\$ anyway; see <https://tex.stackexchange.com/questions/503/why-is-preferable-to> and [https://tex.stackexchange.com/questions/40492/](https://tex.stackexchange.com/questions/40492/what-are-the-differences-between-align-equation-and-displaymath)
 526 [what-are-the-differences-between-align-equation-and-displaymath](https://tex.stackexchange.com/questions/40492/what-are-the-differences-between-align-equation-and-displaymath) for more infor-
 527 mation.)
 528

¹Sample of the first footnote.

²As in this example.

529 **F Final instructions**

530 Do not change any aspects of the formatting parameters in the style files. In particular, do not modify
531 the width or length of the rectangle the text should fit into, and do not change font sizes (except
532 perhaps in the **References** section; see below). Please note that pages should be numbered.

533 **E Preparing PDF files**

534 Please prepare submission files with paper size “US Letter,” and not, for example, “A4.”

535 Fonts were the main cause of problems in the past years. Your PDF file must only contain Type 1 or
536 Embedded TrueType fonts. Here are a few instructions to achieve this.

- 537 • You should directly generate PDF files using `pdflatex`.
- 538 • You can check which fonts a PDF files uses. In Acrobat Reader, select the menu
539 Files>Document Properties>Fonts and select Show All Fonts. You can also use the program
540 `pdffonts` which comes with `xpdf` and is available out-of-the-box on most Linux machines.
- 541 • `xfig` “patterned” shapes are implemented with bitmap fonts. Use “solid” shapes instead.
- 542 • The `\bbold` package almost always uses bitmap fonts. You should use the equivalent AMS
543 Fonts:

544 `\usepackage{amsfonts}`

545 followed by, e.g., `\mathbb{R}`, `\mathbb{N}`, or `\mathbb{C}` for \mathbb{R} , \mathbb{N} or \mathbb{C} . You can also
546 use the following workaround for reals, natural and complex:

```
547 \newcommand{\RR}{I\!\!R} %real numbers  
548 \newcommand{\Nat}{I\!\!N} %natural numbers  
549 \newcommand{\CC}{I\!\!C} %complex numbers
```

550 Note that `amsfonts` is automatically loaded by the `amssymb` package.

551 If your file contains type 3 fonts or non embedded TrueType fonts, we will ask you to fix it.

552 **A Margins in L^AT_EX**

553 Most of the margin problems come from figures positioned by hand using `\special` or other
554 commands. We suggest using the command `\includegraphics` from the `graphicx` package.
555 Always specify the figure width as a multiple of the line width as in the example below:

```
556 \usepackage[pdftex]{graphicx} ...  
557 \includegraphics[width=0.8\linewidth]{myfile.pdf}
```

558 See Section 4.4 in the graphics bundle documentation ([http://mirrors.ctan.org/macros/](http://mirrors.ctan.org/macros/latex/required/graphics/grfguide.pdf)
559 [latex/required/graphics/grfguide.pdf](http://mirrors.ctan.org/macros/latex/required/graphics/grfguide.pdf))

560 A number of width problems arise when L^AT_EX cannot properly hyphenate a line. Please give LaTeX
561 hyphenation hints using the `\-` command when necessary.

562 **F Supplementary Material**

563 Authors may wish to optionally include extra information (complete proofs, additional experiments
564 and plots) in the appendix. All such materials should be part of the supplemental material (submitted
565 separately) and should NOT be included in the main submission.

566 **References**

567 References follow the acknowledgments in the camera-ready paper. Use unnumbered first-level
568 heading for the references. Any choice of citation style is acceptable as long as you are consistent. It

569 is permissible to reduce the font size to small (9 point) when listing the references. Note that the
570 Reference section does not count towards the page limit.

- 571 [1] Alexander, J.A. & Mozer, M.C. (1995) Template-based algorithms for connectionist rule extraction. In
572 G. Tesauro, D.S. Touretzky and T.K. Leen (eds.), *Advances in Neural Information Processing Systems 7*, pp.
573 609–616. Cambridge, MA: MIT Press.
- 574 [2] Bower, J.M. & Beeman, D. (1995) *The Book of GENESIS: Exploring Realistic Neural Models with the*
575 *GENeral NEural Simulation System*. New York: TELOS/Springer-Verlag.
- 576 [3] Hasselmo, M.E., Schnell, E. & Barkai, E. (1995) Dynamics of learning and recall at excitatory recurrent
577 synapses and cholinergic modulation in rat hippocampal region CA3. *Journal of Neuroscience* **15**(7):5249-5262.